

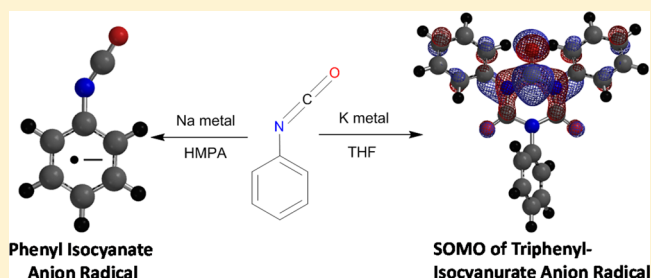
Phenyl Isocyanate Anion Radicals and Their Cyclotrimerization to Triphenyl Isocyanurate Anion Radicals

Mark A. Servos, Nathaniel C. Smart, Mark E. Kassabaum, Cody A. Scholtens, and Steven J. Peters*

Department of Chemistry, Illinois State University, Normal, Illinois 61790-4160, United States

S Supporting Information

ABSTRACT: Room-temperature sodium metal reduction of phenyl isocyanate (PhNCO) in hexamethylphosphoramide yields the anion radical (PhNCO^{•-}) where the unpaired electron exhibits coupling to one nitrogen and five unique protons. The extent of coupling to the carbon in the NCO group was obtained via the reduction of ¹³C-labeled PhN¹³CO. Remarkably, this coupling is over 2 orders of magnitude smaller than that found for the alkyl-substituted analogue. This large attenuation indicates that the electron is not localized within the isocyanate group (as in the alkyl analogues) but is distributed throughout the entire π system including the phenyl ring. The consequence of this delocalization is that the isocyanate is expected to remain linear upon reduction of PhNCO. The anion radicals of *p*-tolyl- and *p*-methoxyphenyl isocyanate have also been generated. We find that these electron-donating substituents on the phenyl ring have little effect on the nitrogen coupling. Hence, the NCO group has the same geometry as the PhNCO^{•-}. When PhNCO is reduced in tetrahydrofuran, a solvent where ion association effects are common, PhNCO^{•-} is not observed. Here, a cyclotrimerization occurs (initiated by PhNCO^{•-}), generating the triphenyl isocyanurate anion radical where the unpaired electron is predominately localized in one of the carbonyl moieties.



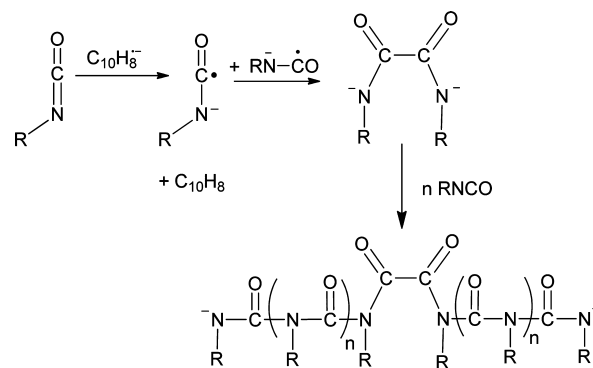
INTRODUCTION

The chemistry of isocyanates (R-NCO) has been extensively explored since their discovery in 1848 by Wurtz,¹ with their greatest use being in the production of polyurethane materials.^{2,3} Moreover, the cyclotrimerization of isocyanates leads to the formation of heterocyclic aromatic isocyanurates (1,3,5-triazinane-2,4,6-triones), which are also commonly used in polyurethane blends giving these materials added resilience.^{4–6} More recently, isocyanates have been widely used in the production of new cyclic lactam precursors as potential antibiotics and protein inhibitors,^{7–11} and for the synthesis of a variety of natural products.^{12–14} Even polyisocyanate macromolecules (e.g., 1-nylon) formed through poly amide bond linkages,^{2,15} have been widely studied as artificial helical polymers that mimic some aspects of protein structure.^{16–20} Due to the unique structural properties of 1-nylon, these polymers have also been exploited for possible use in liquid crystalline materials and as linkers to optical and molecular switches.^{17–22}

Formation of these polyisocyanates is commonly performed using an anionic initiator that attacks the electrophilic carbon of the isocyanate forming an intermediate anion that propagates the polymerization reaction.^{15–18,20} Many of these methods have utilized the formation of an isocyanate anion radical to initiate the polymerization.^{15,16,20} The one-electron reduction of an isocyanate and subsequent polymerization is done using alkali metals or other electron donors (such as the naphthalene anion radical, C₁₀H₈^{•-}) at low temperatures.^{15,16,20} The

mechanism describing polymer formation involves the rapid radical–radical coupling of two isocyanate anion radicals with formation of a diamagnetic oxanilide dianion (Scheme 1). The propagation reaction continues with this dianion species, as a bidirectional polymerization occurs generating two intramolecular polyisocyanate chains attached to the oxanilide moiety, Scheme 1.^{16,20} The high reactivity of isocyanate anion radicals, and their propensity to rapidly polymerize, makes exploring their structure extremely challenging.

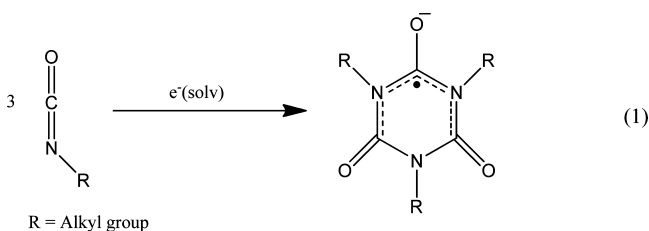
Scheme 1. Formation of Polyisocyanate Initiated by the Coupling of Two Isocyanate Anion Radicals



Received: February 8, 2013

Published: March 31, 2013

Our group recently investigated the one-electron reduction of both ethyl and cyclohexyl isocyanate in dilute solution under ambient conditions in the hope of observing the respective anion radicals, but we were unsuccessful.²³ Instead, the reduced alkyl isocyanate participates in a rapid cyclotrimerization generating a stable trialkyl isocyanurate anion radical, reaction 1.²³ The unpaired electron was found to localize in the π system of one of the carbonyl groups in the ring.



To the best of our knowledge, the only published finding of a stable isocyanate anion radical is that of methyl isocyanate (MeNCO) by Symons and Trousson; however, this was done at exceedingly low temperatures.²⁴ In their studies, the MeNCO^{•-} was generated in a dilute solid solvent matrix of 2-methylTHF or methanol at 77 K using γ -radiation to generate the anion radical. Under these conditions, the anion radical is trapped within the solvent matrix, unable to undergo polymerization, and was readily observable using EPR spectroscopy. They concluded, from the large observed electron coupling to the nitrogen and carbon atoms in the NCO moiety, that the unpaired electron is localized on the carbon atom in MeNCO^{•-} resulting in a bent geometry for the isocyanate group.²⁴ Other than in this study, no spectral data have been observed for any other isocyanate anion radical.

We are particularly interested in generating an isocyanate anion radical for spectroscopic investigation to explore the similarities, if any, with the structure and the electron-spin distribution found in ketyls (e.g., RNCO^{•-} vs R₂CO^{•-}), which are possibly the most important and most investigated class of anion radicals.^{25–40} EPR spectroscopy has been instrumental in understanding the structure of ketyls as well as any perturbation in electron spin density as a consequence of ion association in solvents of varying polarity.^{26,27,29–36} As with MeNCO^{•-}, aliphatic ketyls have the majority of the electron density residing in the carbonyl moiety resulting in a deviation from planarity for the sp²-hybridized carbon.³³ Alternatively, aryl-substituted ketyls have the spin population throughout the extended conjugated π -system resulting in a structure where the ketyl moiety remains planar.⁴⁰ Will the same be true for reduced aryl isocyanates?

The reactivity of ketyls is also well documented, and they have been shown to dimerize under conditions that favor strong ion association to the counteranion.^{26–28,34,36,39} Remarkably, benzophenone ketyl (a commonly used anion radical for the preparation of absolute THF) not only can dimerize but also can undergo hydrogen isotope exchange with THF-*d*₈.³⁸ This exchange appears to be dependent on the alkali metal used (and therefore the degree of ion association) in the one-electron reduction.³⁸ We imagine that ion association is critical to any chemistry involving isocyanate anion radicals (such as polyisocyanate formation) and an understanding of their structure is currently lacking.

Herein, we report the results describing the one-electron reduction of phenyl isocyanate, as well as of three *para*-

substituted phenyl isocyanates, and the first spectroscopic observation of their respective anion radicals. Moreover, it will be shown that the electron spin distribution in the NCO moiety is substantially different from that found for MeNCO^{•-},²⁴ and that solvation effects do play an important role in the chemistry of these newly observed anion radicals.

RESULTS AND DISCUSSION

The sodium metal reduction of phenyl isocyanate (PhNCO, **1**) in hexamethylphosphoramide (HMPA) results in a solution exhibiting a unique EPR spectrum, Figure 1. A nearly perfect

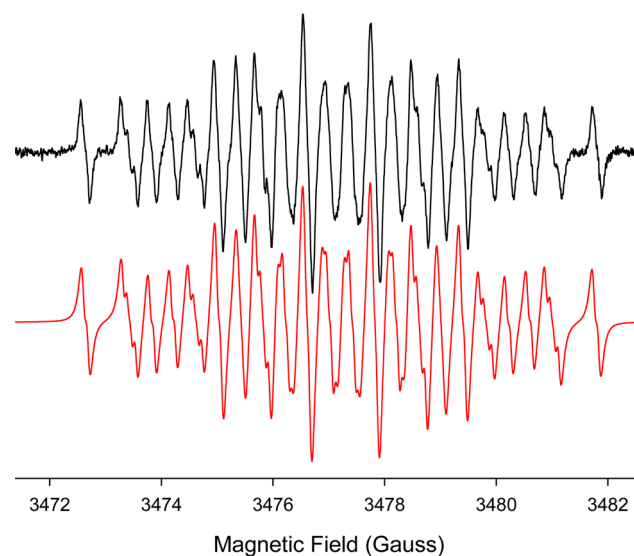


Figure 1. (Upper) X-band EPR spectrum recorded at 295 K after a HMPA solution containing phenyl isocyanate (PhNCO) was exposed to Na metal under vacuum. (Lower) Computer-generated EPR spectrum using a_N of 1.19 G and a_H 's of 2.80, 2.40, 0.860, 0.710, and 0.085 G for five unique protons. The peak-to-peak line width (Δw_{pp}) is 0.09 G.

computer simulation reveals that the odd electron is coupled to five nonequivalent protons and one nitrogen atom, which strongly suggests that the signal is due to the anion radical of phenyl isocyanate (**1**^{•-}). No ion-pairing effects with the Na⁺ cation were observed due to strong solvation by the HMPA.⁴¹ Upon further exposure of this solution to the metal the signal from **1**^{•-} eventually disappears and no other radical was observed during the remainder of the reduction.

A complete picture of the electron-spin density in the isocyanate moiety, especially at the carbon atom, is crucial to predicting the geometry of this anion radical. This was accomplished by reducing ¹³C labeled phenyl isocyanate (PhN¹³CO) that was synthesized from ¹³C enriched benzoic acid (Ph¹³COOH). The Na metal reduction was repeated using a 1:1 mixture of PhNCO/PhN¹³CO in HMPA, and the resulting EPR spectrum clearly shows the additional coupling to the isocyanate ¹³C atom ($a_{13C} = 0.83$ G), Figure 2. Notably, we find that the measured nitrogen and carbon coupling constants for **1**^{•-} are quite different from those found for MeNCO^{•-} determined by Symons and Trousson (e.g., $a_N = 7$ G and $a_{13C} = 110$ G) where they concluded, based upon these large hyperfine couplings, that the electron is localized on the isocyanate carbon and that the NCO takes on a bent geometry upon reduction. However, it is clear from our measured a_N and a_{13C} values for **1**^{•-} that the electron is not localized in the isocyanate

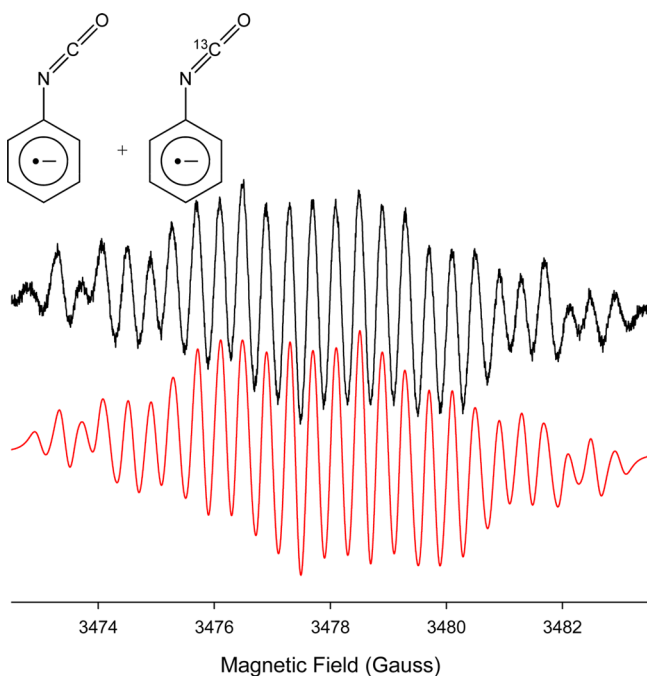


Figure 2. (Upper) EPR spectrum recorded at 295 K of a HMPA solution containing a 1:1 mixture of PhNCO and PhN¹³CO reduced with Na metal. (Lower) Computer-generated EPR spectrum using a 1:1 mixture of two spectra representing the PhNCO^{•-} and PhN¹³CO^{•-}. For both simulated spectra the same coupling constants were used: a_N of 1.19 G for one nitrogen and a_H 's of 2.80, 2.40, 0.860, 0.710, and 0.085 G for five unique protons. An additional coupling, a_{13C} , of 0.83 G was included for one of the simulated spectra. The Δw_{pp} is 0.19 G.

group given that the ¹³C coupling is over 2 orders of magnitude smaller than that found for MeNCO^{•-}.²⁴ This large attenuation in spin density is caused by the extended π conjugation between the isocyanate group and the phenyl ring which allows for greater delocalization of the unpaired electron throughout **1**^{•-}. With substantially less total spin density now residing at the carbon, the geometry for **1**^{•-} is likely to be similar to that of

the neutral molecule where the \angle NCO bond angle remains linear and the \angle CNC remains bent. Moreover, the rotation of the isocyanate group with respect to the phenyl ring must be slow on the EPR time scale causing all five protons to be nonequivalent. Results obtained from density functional theory (DFT) calculations on **1**^{•-} support these conclusions.

Two DFT geometry optimizations were performed for **1**^{•-} both at the B3LYP/6-311++G** level of theory. The initial geometry used for these anion radical calculations was that of the B3LYP/6-31G* optimized structure for **1**. For the first calculation on **1**^{•-} the NCO moiety was kept at the same bond angle as that found for the optimized geometry in **1** (\angle NCO = 174°), while the second calculation had no constraints on the isocyanate group. These results along with the B3LYP/6-311++G**/EPR-II computed Fermi contact electron–nuclear coupling constants (shown in parentheses) are displayed in Figure 3. Interestingly, the optimized geometry where no constraints were used gives the more stable gas phase structure for **1**^{•-} by 53 kJ/mol and contains a bent NCO geometry (\angle NCO = 132°). However, we find with this structure that the calculated a_{13C} and a_N are in very poor agreement with the experimentally determined values (Figure 3) and suggests that the electron will localize in the isocyanate group of **1**^{•-} when formed in the gas phase. Remarkably, by keeping the NCO geometry the same as that obtained for the optimized neutral molecule (e.g., nearly linear), we find that the electron spin is more delocalized into the phenyl π system and that the calculated carbon and nitrogen coupling constants are in good agreement with our measured values, Figure 3. We favor this calculated structure over the former to best resemble **1**^{•-} in solution, which indicates that solvation effects are important to the stability and structure of the phenyl isocyanate anion radical.

The assignment of the measured a_H 's to the five ring hydrogens is also displayed in Figure 3 and is based upon the magnitude of the calculated Fermi contact coupling values where we find better agreement between the measured and calculated a_H 's for the linear isocyanate structure over that for the bent geometry. Furthermore, these assignments are consistent with the results obtained with other similarly

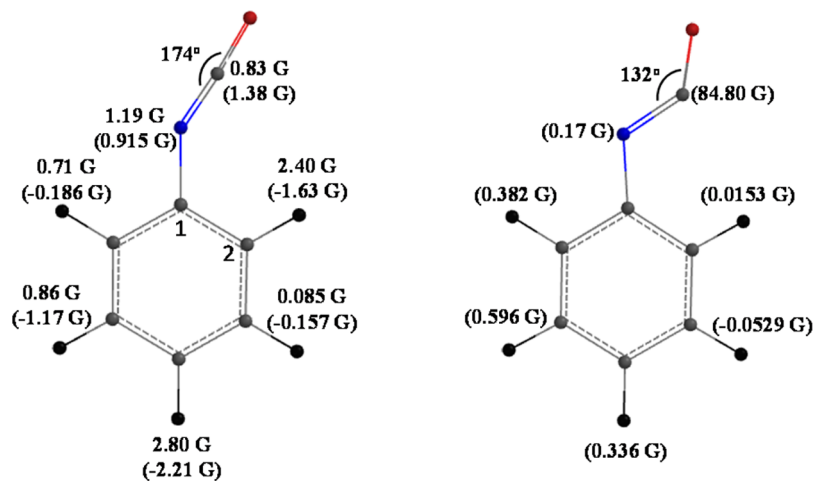


Figure 3. B3LYP/6-311++G**-predicted geometries for two structures of **1**^{•-}. The left structure was obtained by locking the NCO moiety in the same configuration as that obtained for the B3LYP//6-31G* optimized neutral molecule (\angle NCO = 174°), while in the other calculation no restrictions were made to the NCO group (right structure). All measured coupling constants are shown with the left structure along with the 6-311++G**/EPR-II-computed Fermi contact coupling constants (in parentheses) for both calculated **1**^{•-} structures. The assignment of the measured a_H 's to each proton was made based on the magnitude of the DFT calculated values.

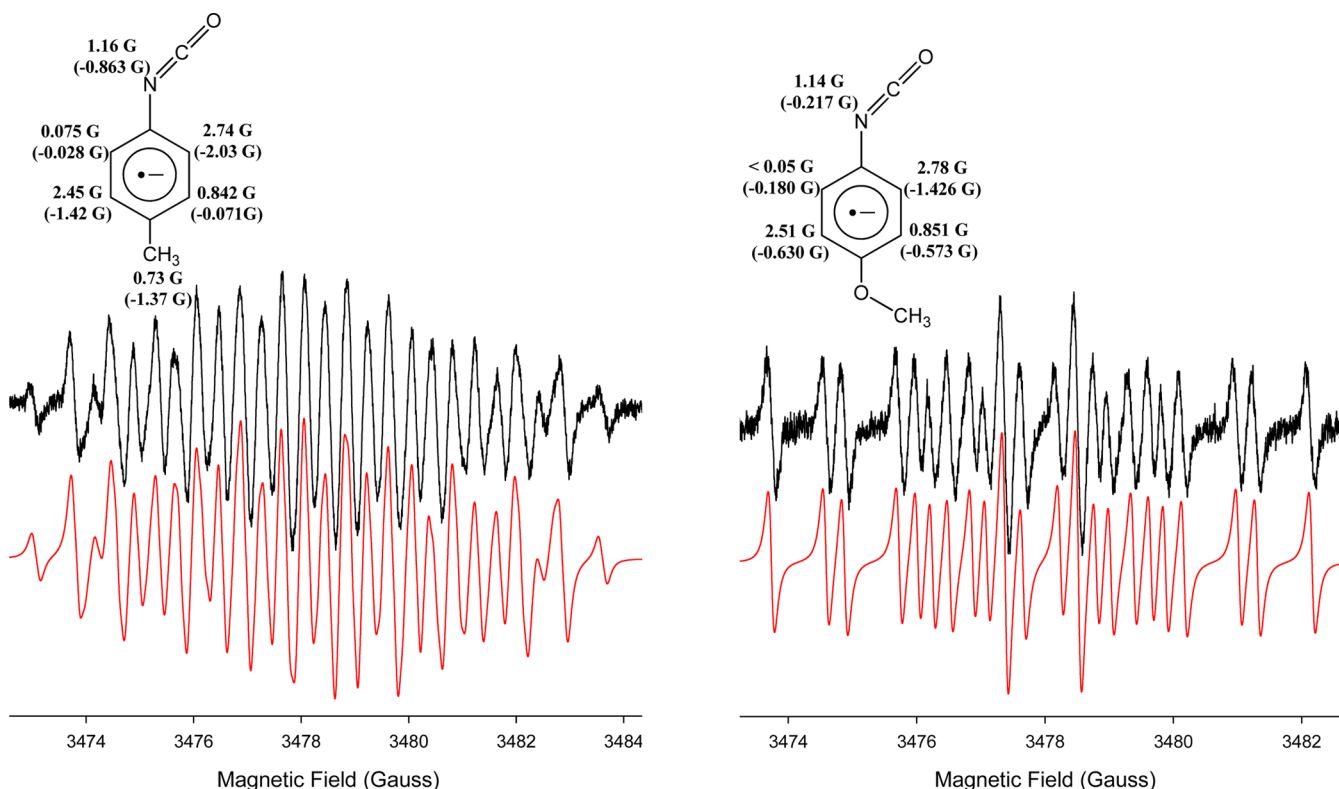


Figure 4. (Left) X-band EPR spectrum recorded at 295 K after a HMPA/*p*-tolyl isocyanate ($2^{\bullet-}$) solution was exposed to Na metal under vacuum. A computer simulation of this spectrum (lower) was generated using an a_N of 1.16 G and a_H 's of 2.74 G (1H), 2.45 G (1H), 0.842 G (1H), 0.075 G (1H), and 0.73 G (3H). The Δw_{pp} is 0.12 G. (Right) EPR spectrum recorded at 295 K after reducing *p*-methoxyphenyl isocyanate in HMPA with Na metal. The computer simulation (lower) was generated using an a_N of 1.14 G and a_H 's of 2.78 G (1H), 2.51 G (1H), 0.851 G (1H). The Δw_{pp} is 0.10 G. Structures shown include the B3LYP//6-311++G**/EPR-II-computed Fermi contact electron–nuclear coupling constants (shown in parentheses).

substituted phenyl anion radicals where the substituent has electron withdrawing characteristics.^{40a,42} The anion radicals of nitrosobenzene and benzaldehyde exhibit larger spin densities in the *ortho* and *para* positions relative to those found for the *meta* positions. We see in the case of $1^{\bullet-}$ that a similar result is obtained where one of the *ortho* and the *para* hydrogens have the largest a_{HS} . Furthermore, a significant difference in the measured a_{HS} for the two *ortho* and the two *meta* hydrogens has been observed for the nitrosobenzene and benzaldehyde anion radicals.^{40a,42} In the case of the latter this difference is 1.29 G (*ortho* positions) and 0.56 G (*meta* positions).^{40a} A similar effect caused by the asymmetric isocyanate group would account for the differences in the observed couplings found in $1^{\bullet-}$ (Figure 3). Interestingly, we conclude from the different proton couplings that the amount of spin density at these positions is significantly smaller than that found for the benzaldehyde ketyl,^{40a} and this would suggest that the NCO is a much weaker electron-withdrawing group.

Placement of a methyl group or methoxy group at the *para* position on phenyl isocyanate appears to have a negligible effect on the nitrogen hyperfine coupling upon reduction; however, significant redistribution of spin density in the ring is evident by the change in coupling to the remaining four protons. We find with the anion radicals of *p*-tolyl isocyanate ($2^{\bullet-}$) and *p*-methoxyphenyl isocyanate ($3^{\bullet-}$) that the presence of these electron-pushing substituents attenuates the nitrogen coupling only slightly from that of the parent $1^{\bullet-}$. The hyperfine couplings to the four ring protons are very similar for both anion radicals. The assignment of each a_H to the different

protons was made using the same computational procedure described for $1^{\bullet-}$ (see Figure 4) even though the calculated a_{HS} are in poor agreement (especially for $3^{\bullet-}$) with the experimental values suggesting that solvation effects are important to the distribution of electron spin (and structure) within these anion radicals. In both systems we see a significant augmentation in the a_H 's for the hydrogens that are *meta* to the isocyanate while coupling to one of the *ortho* protons has lessened considerably.

One-electron reduction experiments were also performed with *p*-nitrophenyl isocyanate, and it was found that the presence of the strongly electron-withdrawing nitro substituent draws much of the electron density away from the isocyanate group resulting in an EPR signal that is similar to those of other *para*-substituted nitrobenzene anion radicals.⁴³ The coupling constants obtained for the *p*-nitrophenyl isocyanate anion radical are: $a_N = 7.78$ G (1 N), $a_N = 0.10$ G (1 N), $a_H = 3.40$ G (2 H), and $a_H = 1.12$ G (2 Hs). The large observed nitrogen coupling, as well as the triplet of triplets due to the proton couplings, is consistent with these anion radicals; see the Supporting Information for EPR spectrum and simulation.

Symons and Trousson also investigated the structure of the methyl isothiocyanate anion radical ($\text{MeNCS}^{\bullet-}$) under similar experimental conditions as that for $\text{MeNCO}^{\bullet-}$ (e.g., low temperature in a solid solvent matrix) and obtained similar spectroscopic results indicating that the electron is localized in the *p* orbital of the isothiocyanate carbon atom.²⁴ Our attempts to generate $\text{PhNCS}^{\bullet-}$ in HMPA were unsuccessful and would

suggest that this anion radical is more susceptible to polymerization than the isocyanate analogue.

Reduction of Phenyl Isocyanate in Tetrahydrofuran.

When the reduction of PhNCO is performed in THF, a solvent where ion association effects are common with anion radicals,⁴⁴ the results are quite different than those obtained in HMPA. As described above, only $\mathbf{1}^{\bullet-}$ was detected when reduction experiments were carried out in HMPA. This was somewhat surprising since the one electron reduction of alkyl isocyanates in HMPA resulted in the formation of isocyanurate anion radicals (see reaction 1).²³ However, when the one-electron reduction of $\mathbf{1}$ is carried out in tetrahydrofuran (THF) the resulting EPR spectrum reveals that a stable isocyanurate anion radical is formed.

The potassium metal reduction of $\mathbf{1}$ in THF gives a solution that exhibits a strong EPR signal with a 1:2:3:2:1 pentet from the unpaired electron coupling to two equivalent nitrogen atoms ($a_N = 1.37$ G), Figure 5. No signal from $\mathbf{1}^{\bullet-}$ was detected

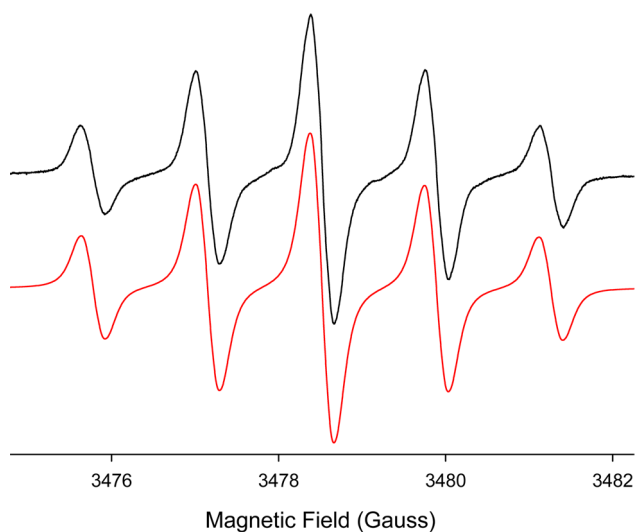


Figure 5. (Upper) EPR spectrum recorded at 295 K after a THF solution containing phenyl isocyanate was exposed to K metal under vacuum. (Lower) Computer-generated EPR spectrum using a_N of 1.37 G (2 Ns) and a_H of 0.080 G (6 Hs) with $\Delta w_{pp} = 0.14$ G.

under these conditions, which suggests that this anion radical is much more reactive in solvents of lower polarity.⁴⁵ In generating a computer simulation of this spectrum it was necessary to include a small unresolved coupling from hydrogens in two of the phenyl rings ($a_H = 0.080$ G, 6 Hs), Figure 5. Six hydrogens were used in the simulation since the majority of spin density in the rings attached to the two Ns is expected to reside at the *ortho* and *para* positions.^{40a,42} Further proof of this unresolved proton splitting was obtained via the reduction of penta-deuteriophenyl isocyanate (Ph(²H₅)NCO, $\mathbf{1-D}_5$). By replacing the ¹Hs on the phenyl rings with ²Hs, a noticeable decrease in the apparent peak width should occur since the ratio of gyromagnetic ratios is, $\gamma_H/\gamma_N = 0.154$, and therefore, any coupling to ²Hs will be lost in the spectral line width.⁴⁶ Figure 6 contains the EPR spectrum obtained from the one-electron reduction of $\mathbf{1-D}_5$ using experimental conditions identical to those used with $\mathbf{1}$; as expected, the spectral peak width is much narrower when compared to the EPR spectrum in Figure 5. Clearly these results show that very little spin density is distributed into the phenyl rings of the anion radical formed.

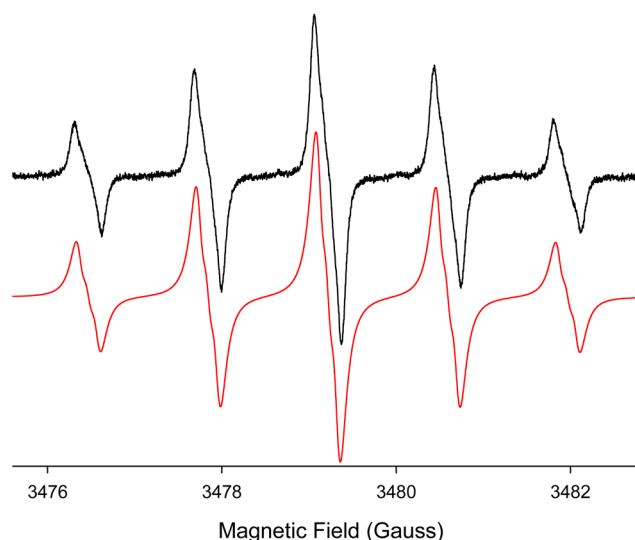


Figure 6. (Upper) EPR spectrum recorded at 295 K after a THF solution containing Ph(²H₅)NCO was exposed to K metal. (Lower) Computer simulation using $a_N = 1.37$ G (2 Ns) and $a_N = 0.095$ G (1 N) and $\Delta w_{pp} = 0.12$ G.

Upon closer inspection of the spectrum shown in Figure 6 we find that the pentet exhibits further splitting due to a third nitrogen ($a_N = 0.095$ G). This splitting is not from any deuterium atoms since $a_H \cong 0.012$ G ($a_H \times 0.154$), and therefore any coupling (even to six ²Hs) would be lost in the spectral line width. As further evidence that an isocyanurate anion radical has formed in solution, the reduction of PhN¹³CO was also performed and the resulting spectrum clearly exhibits additional couplings to only three carbons with $a_{13C} = 1.52$ G (1 \times ¹³C) and $a_{13C} = 0.835$ G (2 \times ¹³C), Figure 7. The observed coupling to 3 N's and 3 ¹³C's, as well as the

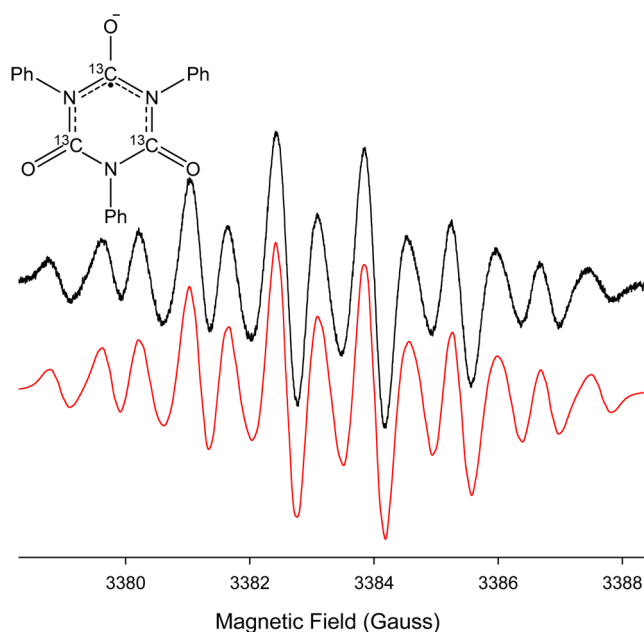
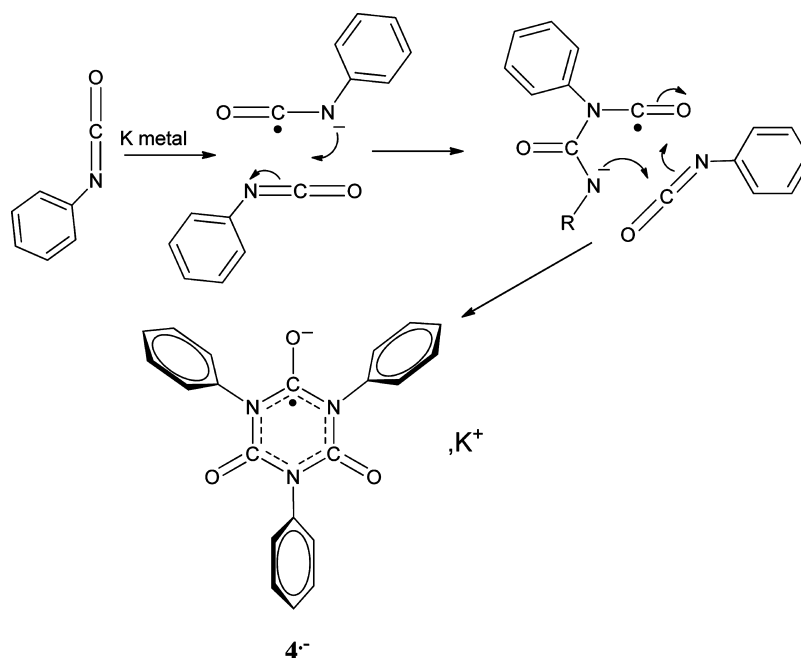


Figure 7. (Upper) EPR spectrum recorded at 295 K after a THF solution containing PhN¹³CO was exposed to K metal. (Lower) Computer-generated EPR simulation using $a_N = 1.38$ G (2 Ns), $a_{13C} = 1.52$ G (1 ¹³C), $a_{13C} = 0.835$ G (2 ¹³Cs) and $a_H = 0.10$ G (6 Hs), $\Delta w_{pp} = 0.15$ G.

Scheme 2. Potassium Metal Reduction of a THF/PhNCO Solution Resulting in a Rapid Cyclotrimerization and the Formation of the Triphenyl Isocyanurate Anion Radical



symmetrical nature of these couplings, leaves little doubt that the anion radical was generated from a cyclotrimerization of three PhN¹³CO molecules. The electron-spin distribution within this trimer is nearly identical to that observed in the reduction of trialkyl isocyanurates,²³ which also strongly supports the formation of the triphenyl isocyanurate anion radical (4^{•-}) upon reduction of 1 in THF. Moreover, we envision that a cyclotrimerization mechanism, initiated by 1^{•-}, drives the rapid formation of the trimer anion radical, Scheme 2. Finally, upon oxidation of the reduced THF solution with iodine, ¹H and ¹³C{¹H} NMR spectroscopy were used to determine that 4 was the major species (~93%) found in solution. As was observed with the trialkyl isocyanurate anion radicals,²³ the electron spin in 4^{•-} is predominately localized within the π system of one of the three carbonyls.

B3LYP/6-31G* calculations on both 4 and 4^{•-} suggest that the neutral molecule will undergo a significant structural rearrangement once an electron is added to the π system. The structure of 4 has D_{3h} symmetry where the phenyl rings are orthogonal to the planar isocyanurate ring, Figure 8. These calculations also indicate that the isocyanurate ring in 4 must undergo a first order Jahn–Teller (J–T) distortion and lose of planarity upon electron attachment. This distortion reduces the symmetry of the ring in 4^{•-} which now has a nonplanar geometry (C_s symmetry) where the carbonyl with high spin density is now slightly pyramidalized. The decrease in symmetry upon addition of an electron means that two or more deformed structures (or J–T species) must be present which can undergo rapid exchange.⁴⁷ In the EPR data, we observe only one J–T species in solution, even at low temperatures, but this may be the result of a dynamic J–T effect between the different conformers that interchange rapidly on the EPR time scale.⁴⁷

We performed a conformational search of other possible J–T species involving the isocyanurate ring. These calculations were performed using the less structurally complex trimethyl isocyanurate anion radical where conformers of the isocyanurate

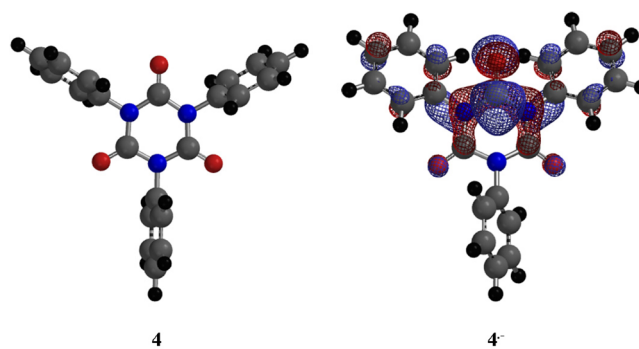


Figure 8. B3LYP/6-31G*-predicted geometries for 4 and 4^{•-}. Structure 4 has D_{3h} symmetry where the plane of the phenyl rings is orthogonal to the planar isocyanurate ring. In the case of 4^{•-} the isocyanurate is no longer flat and the carbonyl with high electron density is slightly pyramidalized. Note that the phenyl rings adjacent to this carbonyl have rotated to become somewhat coplanar with the isocyanurate moiety. Also shown is the shape of the π -SOMO surface for 4^{•-}, which supports the experimental result that the electron is localized in one carbonyl.

rate ring could be readily found. The lowest energy conformer of the trimethyl isocyanurate anion radical has nearly the same geometry, π -SOMO and spin distribution for the isocyanurate ring as that found for 4^{•-}. Two other possible conformers were found and their structures are shown in Supporting Information.

We see from the optimized structure for 4^{•-} (Figure 8) that two of the phenyl rings have become almost coplanar with that of the isocyanurate ring. This structure allows for increased π orbital overlap between the rings as well as increased spin density into the two phenyl rings. On the whole, the shape of the π -SOMO surface for 4^{•-} conforms remarkably well to the magnitude of the coupling constants (and therefore the electron spin density) observed for the carbons and nitrogens in the isocyanurate ring.

Attempts were made to reduce **4** directly in THF; however, no anion radical was detected via EPR, and NMR analysis revealed that **4** was still present in solution. It was apparent in these experiments that the metal became covered by a thin-film residue and that this film likely inactivated the metal surface. Even exposure to solvated electron in THF (generated with 18-crown-6 ether) did not form $4^{\bullet-}$; instead, complete decomposition of **4** occurs as evident in the NMR data. Further experimental techniques are currently being explored (e.g., cyclic voltammetry) to attempt to reduce **4**, as well as other aryl-substituted isocyanurate compounds. However, we surmise that the reaction pathway described in Scheme 2 circumvents this difficulty, which has made it possible to obtain $4^{\bullet-}$ in solution starting with $1^{\bullet-}$.

Tight ion pairing is clearly evident with some isocyanurate anion radicals which exhibit coupling to the metal cation. Notably, the degree of ion pairing has a noticeable influence on the hyperfine coupling to the nitrogen and carbon atoms in these systems. In the case of the triethyl isocyanurate anion radical, $5^{\bullet-}$ (Figure 9), a tight ion pair exists in solution even

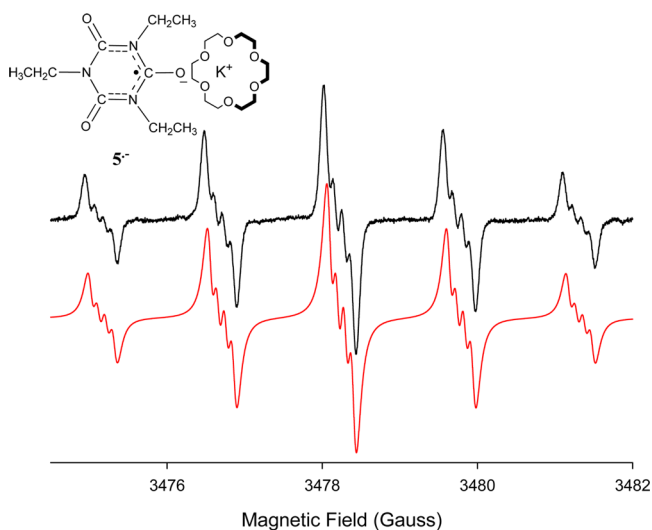
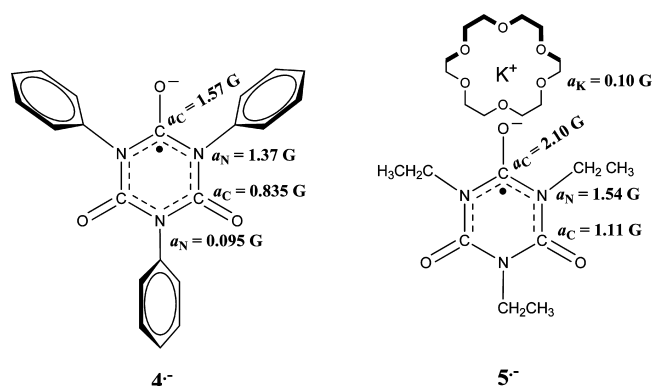


Figure 9. (Upper) EPR spectrum of a THF solution containing 1.5:1 mixture of EtNCO/18-crown-6 ether after exposure to K metal at 295 K. (Lower) Computer-generated EPR spectrum using $a_N = 1.54$ G (2 N) and $a_K = 0.10$ G (1 K), $\Delta w_{pp} = 0.10$ G.

when the K^+ is encapsulated in an 18-crown-6 ether. (The EPR spectrum exhibits hyperfine coupling to the K^+ nucleus ($I = 3/2$), $a_K = 0.10$ G.) This tight (or contact) ion pair likely involves the oxygen that has the majority of charge density within the isocyanurate ring, see Figure 9. Alternatively, no metal splitting is apparent for the anion radical of $4^{\bullet-}$ (see Figures 3 and 4), and therefore a loose or solvent separated ion pair must exist where it is likely the phenyl rings are sterically inhibiting the K^+ from forming a contact ion pair with the negatively charged carbonyl group. These differences in ion association result in a measurable difference in the nitrogen and carbon hyperfine coupling constants in $4^{\bullet-}$ and $5^{\bullet-}$. Although the electron is predominately localized in one carbonyl for both anion radicals, we find that the contact ion pair formed with $5^{\bullet-}$ has more electron density in the carbonyl, which is apparent when comparing the nitrogen and carbon hyperfine couplings with those found for the loose ion pair ($4^{\bullet-}$), see Structures $4^{\bullet-}$ and $5^{\bullet-}$. (Supporting Information contains the EPR spectrum of ^{13}C labeled $5^{\bullet-}$ along with the computer generated simulation).

In the case of $4^{\bullet-}$, an increase in electron distribution throughout the ring allows for more spin density to reside on the remaining nitrogen and enhances our ability to observe the small hyperfine coupling ($a_N = 0.095$ G), Figure 6.



CONCLUSION

The reduction of phenyl isocyanate, under conditions where ion association is typically absent (e.g., in HMPA), leads to the formation of the respective anion radical where the electron is not localized on the carbon in the isocyanate group but is distributed throughout the π system. The magnitude of the carbon- and nitrogen-coupling constants as well as DFT calculations reveal that the isocyanate group remains linear in these anion radicals (as in the neutral molecule). Alternatively, when the reduction is carried out under conditions where ion association is likely to occur, no isocyanate anion radical is observed. Instead, we find that a rapid cyclotrimerization, initiated by the isocyanate anion radical, takes place resulting in the formation of an isocyanurate anion radical. Finally, ion pairing effects result in a noticeable perturbation in the electron-spin distribution throughout the isocyanurate ring. This methodology for reducing isocyanates represents a convenient way to study the chemistry of these anion radicals and to see how different substituents attached to the isocyanate moiety influence the reduction chemistry.

EXPERIMENTAL SECTION

Materials. ^{13}C -Benzoic acid ($C_6H_5^{13}COOH$) and perdeuterated benzoic acid ($Ph(^2H_5)COOH$) were purchased from Cambridge Isotopes, Inc., and used in the synthesis of the respective isocyanates.

Synthesis of ^{13}C -Phenyl Isocyanate ($Ph^{13}CO$) and Perdeuterated Phenyl Isocyanate ($Ph(^2H_5)NCO$). A mixture of 8.2 mmol of $Ph^{13}COOH$ (or $Ph(^2H_5)COOH$) and 10.4 mmol of $SOCl_2$ was dissolved in 50 mL of CH_2Cl_2 . The solution was refluxed for 8 h under an argon atmosphere after which the CH_2Cl_2 was distilled off, leaving the crude benzoyl chloride ($Ph^{13}COCl$) behind. To the flask containing $Ph^{13}COCl$ were added 30 mL of benzene and 50 mL of an aqueous solution containing a large excess of NaN_3 (34 mmol). This solution was stirred vigorously to maximize the mixing of both layers. Aliquots of the benzene solution were removed and interrogated using GCMS to monitor the complete conversion of $Ph^{13}COCl$ to the acyl azide ($Ph^{13}CON_3$). The conversion took approximately 24 h. After this time, the benzene layer was separated from the aqueous layer and dried with anhydrous $MgSO_4$. The filtered benzene solution containing $Ph^{13}CON_3$ was refluxed for 6 h under argon to drive the conversion of the acyl azide to the isocyanate via a Curtius rearrangement. The benzene was then removed and the crude product ($PhN^{13}CO$) was distilled under reduced pressure (18 Torr) at $71^\circ C$. $^{13}C\{^1H\}$ NMR spectral analysis confirm the formation of the isocyanate, Figure 10. The same procedure was used to synthesize

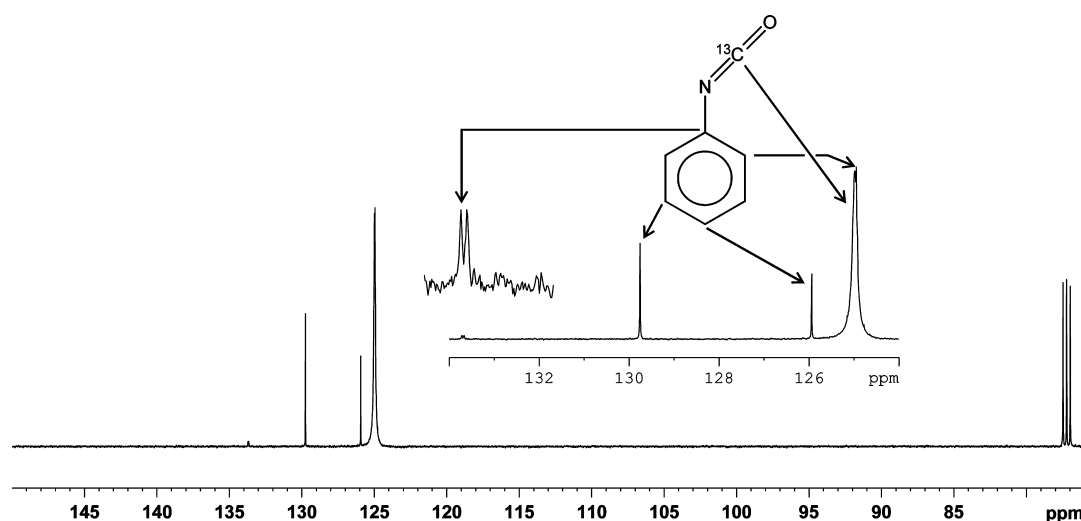


Figure 10. 125 MHz $^{13}\text{C}\{^1\text{H}\}$ NMR spectrum of PhN^{13}CO in CDCl_3 . Note that the ipso carbon resonance is split by coupling to the isocyanate carbon ($^2J_{\text{CC}} = 6.3$ Hz).

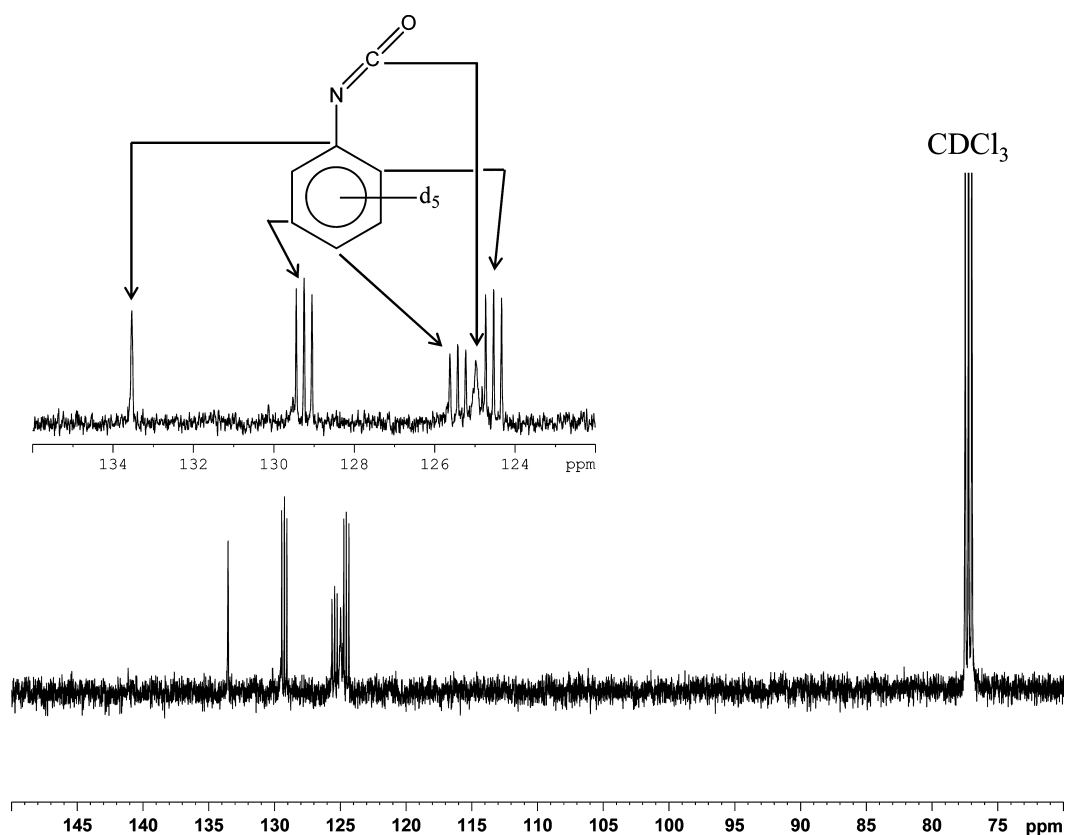


Figure 11. 125 MHz $^{13}\text{C}\{^1\text{H}\}$ NMR spectrum of synthesized $\text{Ph}(^2\text{H}_3)\text{NCO}$ in CDCl_3 . Note the carbon resonances that are split into a triplet by the deuterium ($I = 1$) attached.

$\text{Ph}(^2\text{H}_3)\text{NCO}$ and the $^{13}\text{C}\{^1\text{H}\}$ NMR spectrum is displayed in Figure 11.

Reduction of Phenyl Isocyanate Compounds in HMPA and THF. A sealed glass tube (with fragile ends) was charged with 0.15 mmol of phenyl isocyanate and placed into bulb E of the Pyrex glass apparatus shown in Figure 12. A small amount of either sodium or potassium metal was placed into bulb B, which was then sealed at point A, and the entire apparatus was evacuated. The alkali metal was distilled into bulb D to form a pristine metal mirror, after this, bulb B was sealed at point C. Three milliliters of HMPA (dried with potassium metal) or THF (dried over NaK) were distilled from the

vacuum system directly into bulb E, and the evacuated apparatus was sealed from the vacuum line at point F. The glass tube containing the isocyanate was broken by shaking, and the solution was well mixed before brief exposure to the metal mirror.

The EPR spectrum was immediately recorded after pouring a sample of the solution into the 3 mm EPR tube. The apparatus was removed from the EPR instrument and the solution exposed to more metal and the spectrum recorded again. This process was continued until the best signal-to-noise ratio for the anion radical was obtained. All EPR data was collected on a Bruker EMX-080 spectrometer equipped with a variable-temperature unit.

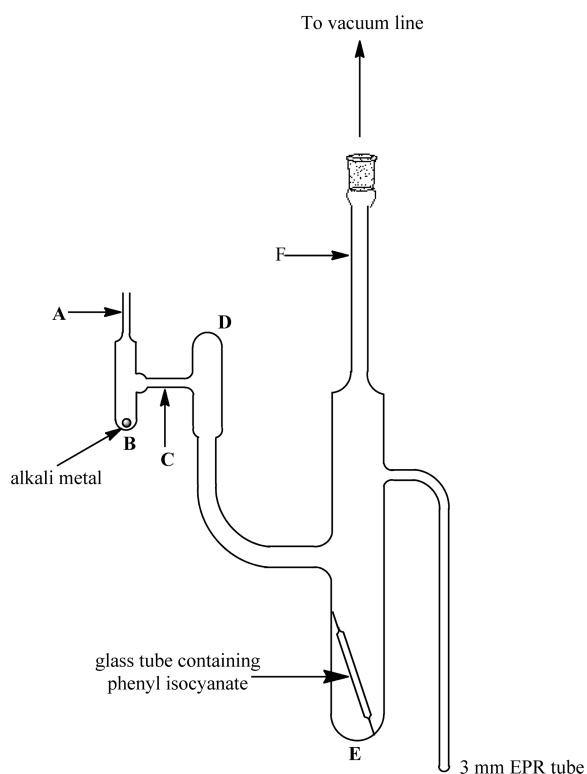


Figure 12. Apparatus used for the generation of the isocyanate and isocyanurate anion radicals in HMPA or THF.

■ ASSOCIATED CONTENT

📄 Supporting Information

Additional EPR spectral data and DFT calculation results. This material is available free of charge via the Internet at <http://pubs.acs.org>.

■ AUTHOR INFORMATION

Corresponding Author

*E-mail: sjpeter@illinoisstate.edu.

Notes

The authors declare no competing financial interest.

■ ACKNOWLEDGMENTS

We thank the American Chemical Society-Petroleum Research Fund (ACS-PRF 51677-UR4) and Illinois State University for funding of this work.

■ REFERENCES

- (1) Wurtz, A. *Compt. Rend.* **1848**, *27*, 241–243.
- (2) Ulrich, H. *Chemistry and Technology of Isocyanates*; John Wiley and Sons: New York, 1996.
- (3) Delebecq, E.; Pascault, J.; Boutevin, B.; Ganachaud, F. *Chem. Rev.* **2013**, *113*, 80–118.
- (4) Raffel, B.; Loevenich, C. J. *J. Cell. Plast.* **2006**, *42*, 17–47.
- (5) Loevenich, C. J.; Raffel, B. *J. Cell. Plast.* **2006**, *42*, 289–305.
- (6) Zitinkina, A. K.; Sibanova, N. A.; Taronkonov, O. G. *Russ. Chem. Rev.* **1985**, *54*, 1866–1898.
- (7) Huard, K.; Bagley, S. W.; Menhaji-Klotz, E.; Preville, C.; Southers, J. A.; Smith, A. C.; Edmonds, D. J.; Lucas, J. C.; Dunn, M. F.; Allanson, N. M.; Blaney, E. L.; Garcia-Irizarry, C. N.; Kohrt, J. T.; Griffith, D. A.; Dow, R. L. *J. Org. Chem.* **2012**, *77*, 10050–10057.
- (8) Fisher, J. F.; Meroueh, S. O.; Mobashery, S. *Chem. Rev.* **2005**, *105*, 395–424.

- (9) Rigby, J. H.; Brouet, J.; Burke, P. J.; Rohach, S.; Sidique, S.; Heeg, M. J. *Org. Lett.* **2006**, *8*, 3121–3123.
- (10) Roberson, C. W.; Woerpel, K. A. *J. Am. Chem. Soc.* **2002**, *124*, 11342–11348.
- (11) Barrett, A. G. M.; Betts, M. J.; Fenwick, A. *J. Org. Chem.* **1985**, *50*, 169–175.
- (12) Rigby, J. H.; Shyama, S. *Org. Lett.* **2007**, *9*, 1219–1221.
- (13) Lei, A.; Lu, X. *Org. Lett.* **2000**, *2*, 2357–2360.
- (14) Brandi, A.; Cicchi, S.; Cordero, F. M. *Chem. Rev.* **2008**, *108*, 3988–4035.
- (15) Shashoua, V. E.; Sweeny, W.; Tietz, R. F. *J. Am. Chem. Soc.* **1960**, *82*, 866–873.
- (16) Bur, A. J.; Fetters, L. J. *Chem. Rev.* **1976**, *76*, 727–746.
- (17) Green, M. M.; Peterson, N. C.; Sato, T.; Teramoto, A.; Cook, R.; Lifson, S. *Science* **1995**, *268*, 1860–1866.
- (18) Green, M. M.; Park, J.-W.; Sato, T.; Teramoto, A.; Lifson, S.; Selinger, R. L. B.; Selinger, J. V. *Angew. Chem., Int. Ed.* **1999**, *38*, 3138–3154.
- (19) Satoh, T.; Ihara, R.; Kawato, D.; Nishikawa, N.; Suemasa, D.; Kondo, Y.; Fuchise, K.; Sakai, R.; Kakuchi, T. *Macromolecules* **2012**, *45*, 3677–3686.
- (20) Shah, P. N.; Min, J.; Chae, C.; Nishikawa, N.; Suemasa, D.; Kakuchi, T.; Satoh, T.; Lee, J. *Macromolecules* **2012**, *45*, 8961–8969.
- (21) Zhao, W.; Kloczkowski, A.; Mark, J. E.; Erman, B.; Bahar, I. *Macromolecules* **1996**, *29*, 2796–2804.
- (22) Pijper, D.; Jongejan, M. G. M.; Meetsma, A.; Feringa, B. L. *J. Am. Chem. Soc.* **2008**, *130*, 4541–4552.
- (23) Peters, S. J.; Klen, J. R.; Smart, N. S. *Org. Lett.* **2008**, *10*, 4521–4524.
- (24) Symons, M. C.; Trousson, P. M. *Radiat. Phys. Chem.* **1984**, *23*, 127–135.
- (25) Lown, J. W. *Can. J. Chem.* **1965**, *43*, 2571–2575.
- (26) Evans, A. G.; Evans, J. C.; Hodden, E. H. *J. Chem. Soc. B* **1969**, 546–547.
- (27) Chen, K. S.; Mao, S. W.; Nakamura, K.; Hirota, N. *J. Am. Chem. Soc.* **1971**, *93*, 6004–6013.
- (28) Staples, T. L.; Szwarc, M. *J. Am. Chem. Soc.* **1970**, *92*, 5022–5027.
- (29) Russell, G. A.; Wallraff, G.; Gerlock, J. L. *J. Phys. Chem.* **1978**, *82*, 1161–1168.
- (30) Nakamura, K. *J. Am. Chem. Soc.* **1981**, *103*, 6973–6974.
- (31) Echevoyen, L.; Neves, I.; Stevenson, C. D. *J. Phys. Chem.* **1982**, *82*, 1611–1614.
- (32) Hirayama, M.; Ohhata, H. *Bull. Chem. Soc. Jpn.* **1987**, *60*, 2751–2756.
- (33) Davies, A. G.; Neville, A. G. *J. Chem. Soc., Perkin Trans. 2* **1992**, 163–169.
- (34) Candida, M.; Shohoji, B. L. *Tetrahedron Lett.* **1995**, *36*, 6167–6170.
- (35) Stevenson, C. D.; Reiter, R. C.; Burton, R. D.; Halvorsen, T. D. *Inorg. Chem.* **1995**, *34*, 1368–1372.
- (36) Scholz, M.; Gescheidt, G.; Daub, J. *J. Chem. Soc., Chem. Commun.* **1995**, 803–804.
- (37) Micha-Screttas, M.; Heropoulos, G. A.; Steele, B. R. *J. Chem. Soc., Perkin Trans. 2* **1999**, 2685–2690.
- (38) Kamaura, M.; Hanamoto, T.; Kuwatani, Y.; Inanaga, J. *J. Am. Chem. Soc.* **1999**, *121*, 6320–6321.
- (39) Macias-Ruvalcaba, N. A.; Felton, G. A. N.; Evans, D. H. *J. Phys. Chem. C* **2009**, *113*, 338–345.
- (40) (a) Steinberger, N.; Fraenkel, G. K. *J. Chem. Phys.* **1964**, *40*, 723–729. (b) Rieger, P. H.; Fraenkel, G. K. *J. Chem. Phys.* **1962**, *37*, 2811–2832.
- (41) Levin, G.; Jagur-Grodzinski, J.; Szwarc, M. *J. Am. Chem. Soc.* **1970**, *92*, 2268–2275. We did find ion pairing effects with the alkyl isocyanurate anion radicals and the Na⁺ cation in our previous studies involving the reduction of alkyl isocyanates; see ref 23.
- (42) Ayscough, P. B.; Sargent, F. B.; Wilson, R. *J. Chem. Soc. B* **1966**, 903–906.

(43) Stevenson, C. D.; Echegoyen, L. *J. Phys. Chem.* **1973**, *77*, 2339–2342.

(44) (a) Ayscough, P. B.; Wilson, R. *Proc. Chem. Soc.* **1962**, 229–230.

(b) Canters, G. W.; De Boer, E. *Mol. Phys.* **1973**, *26*, 1185–1198.

(c) Peters, S. J.; Turk, M. R.; Kiesewetter, M. K.; Reiter, R. C.; Stevenson, C. D. *J. Am. Chem. Soc.* **2003**, *125*, 11212–11213.

(45) The same EPR results were obtained when *p*-tolyl isocyanate and *p*-methoxy isocyanate were reduced under these conditions.

(46) Wertz, J. E.; Bolton, J. R. *Electron Spin Resonance Elementary Theory and Practical Applications*; Chapman and Hall: New York, 1986.

(47) For a discussion and examples of systems that undergo J–T distortion upon electron addition, see: (a) Jahn, H. A.; Teller, E. *Proc. R. Soc. London Ser. A* **1937**, *161*, 220. (b) Horvat, D. A.; Hammons, J. H.; Stevenson, C. D.; Borden, W. T. *J. Am. Chem. Soc.* **1997**, *119*, 9523–9526. (c) Kurth, T. L.; Brown, E. C.; Hattan, C. M.; Reiter, R. C.; Stevenson, C. D. *J. Phys. Chem. A* **2002**, *106*, 478–481. (d) Gerson, F.; Huber, W. *Electron Spin Resonance Spectroscopy of Organic Radicals*; Wiley-VCH: Weinheim, 2003; p 161.